Numerical Study of a UAV with Tandem Wing under Gust Load Influence using Two-Way Fluid-Structure Interaction Method

PARLINDUNGAN, David Waldo, AKBAR, Mahesa and MOELYADI, Mochammad Agoes

International Journal of Technology

http://ijtech.eng.ui.ac.id

Research Article

Numerical Study of a UAV with Tandem Wing under Gust Load Influence using Two-Way Fluid-Structure Interaction Method

David Waldo Parlindungan [1], Mahesa Akbar [1], Mochammad Agoes Moelyadi [1,*]

[1]Faculty of Mechanical and Aerospace Engineering, Institut Teknologi Bandung, Jalan Ganesa 10, Bandung 40132, Indonesia
[*]Corresponding author: moelyadi@itb.ac.id; Tel.: +628112209768

Abstract: This paper presents a new investigation of a tandem wing configuration under cruise and gust load conditions. A wing of a high-altitude long-endurance unmanned air vehicle (HALE UAV) is used as a case study. A two-way fluid-structure interaction (FSI) analysis is conducted. A numerical investigation is done by coupling the Computational Fluid Dynamics (CFD) and Computational Structural Dynamic (CSD) domains. A complex phenomenon is evaluated, i.e., flow interaction between front and rear wings. In addition, the structural response of the rear wing due to the gust disturbance and the interference of downstream flow from the front wing is studied. The variance of gust disturbance is based on the chance of occurrence. The results pointed out that for a more realistic, small gust with higher gust probability, the pattern of the structural response closely follows the gust pattern, i.e., the response reaches its peak similar to the gust shape. However, for a smaller chance of gust, i.e., higher gust amplitude, the structural response has some discrepancies and depicts a sharper trend toward its peak value due to a high change of angle of attack.

Keywords: Computational fluid dynamics; Computational structural dynamics; Fluid-structure interaction; Gust load; Tandem wing

1. Introduction

Environmental impacts of aviation are becoming one of the main challenges in aircraft technology development. Advanced technologies are designed to support a more sustainable flight; thus, there is a strong drive to explore unconventional aircraft (Bravo-Mosquera et al., 2022). Unconventional aircraft configurations, such as canards, flying wings, and tandem wings, hold great promise due to their extraordinary performance characteristics, particularly high aerodynamic efficiency. However, those aircraft are often seen having several issues, mainly with flight stability (Goetzendorf-Grabowski, 2023). Furthermore, some works have elaborated on how the changes in an unconventional wing configuration affected the aeroelastic characteristics, i.e., flutter boundaries (Dhital et al., 2022).

The tandem wing configuration has attracted many researchers for decades as an option to provide an exceptional aerodynamic performance. One of the most famous tandem-wing aircraft, Proteus, developed by NASA and Scaled Composites, demonstrates excellent aerodynamic efficiency at a high-altitude operation (D'Oliveira et al., 2016). Often, to achieve high aerodynamic

This work was supported by the Department of Mechanical and Aerospace Engineer Institut Teknologi Bandung funded by Research, Community Service and Innovation (P2MI ITB) 235A/IT1.C04/DK/KP/2022

https://doi.org/10.14716/ijtech.v16i2.6289
Received December 2022; Revised January 2023; Accepted June 2023

efficiency, a slender, long-span, and high aspect ratio wing is considered. However, a long span is known to have a critical aeroelastic instability, i.e., low divergence speed. One infamous accident is the failure of NASA Helios UAV due to divergence, an aeroelastic condition where the wing has very large deformation (Noll et al., 2004). A tandem wing configuration reduces the aircraft wingspan but still maintains very high aerodynamic efficiency.

Feistel et al. (1981) conducted an investigation on a canard-wing configuration in a wind tunnel. It was one of the earliest published works that observed the effect of tip vortex generated from a front wing (canard). The work by Khan and Mueller (1991) also investigated the effect of wake from a finite canard wing using a Wortmann FX63-137 airfoil. Their experimental results showed that the existence of canard provided a reduction in the downstream drag coefficient, hence, it generated a better aerodynamic efficiency of up to 40% compared to a single wing. Another work by Scharpf and Mueller (1992) conducted an investigation for a two-dimensional airfoil in tandem. Their results also showed that a tandem configuration led to a decrease in drag and a better lift-to-drag ratio. In recent years, studies on tandem wing by means of understanding its effect to the aircraft performance have been conducted (Qin et al., 2024; Chou et al., 2013).

Numerical investigation by means of Reynold-Averaged Navier Stokes (RANS) via commercial software also depicted a promising result in increasing the lift for the tandem airfoils for various applications, i.e., MAV and UAV (Abbey et al., 2020). One of the most recent studies by Shah and Ahmed (2022) investigated the effect of spacing between the tandem wings. The flow generated between the front and rear wings affects each other, especially when the horizontal distance between them is in minimum proximity. Dhital et al. (2022) also evaluated the effect of proximity for another unconventional wing, biplane configuration. Interesting findings were found as the gap between the wings affecting the aeroelastic instability. A smaller gap increased the aerodynamic interaction and decreased the flutter boundary. In recent years, studies on tandem flexible wing or flapping wing by means of computational analysis have been discussed in various articles (Muriel et al., 2024; Yang et al., 2024; Bie and Lie, 2022; Arranz et al., 2020; Broering and Liang, 2015). Most of the studies found that, the aerodynamics and structural responses of the hindwings are affected by intensity of the vortices shed into the wake. Despite this fact, there are only a few published articles discussing the aeroelastic or FSI effect concerning flexible tandem wings.

Most of the studies on the FSI phenomenon, i.e., vortex and wake effect, on tandem configuration, investigated a wing section with spring-like or pendulum-like support to represent elastic movement, i.e., pitching, heaving, or flapping motion (Kirschmeier and Bryant, 2018; Gong et al., 2016). Jones et al. (2015) are among the few researchers who elaborated on the FSI phenomenon in a flexible tandem configuration. They conducted experimental investigations on two combinations of Rigid-Rigid wings and Flexible-Rigid wings. On the Flexible-Rigid wings, it was found that the magnitude of the unsteady aerodynamic forces was influenced by the vortex shedding frequency which coupled with the wing vibration.

In the present study, an effort to investigate the aeroelastic or FSI phenomenon on a tandem wing configuration is conducted. In contrast with the one observed by Jones et al. (2015), instead of a flexible front wing, in this work, a flexible rear wing will be evaluated. The effect of wake from the front wing concerning the vibration of the rear wing is elaborated. In the field of aeroelasticity, potential function-based methods, i.e., Doublet Lattice Method (DLM) and Vortex-Lattice Method (VLM) have been established to model the unsteady aerodynamic loads. Advanced use of DLM coupled with FEM for the aeroelasticity model could be seen in the fields of vibration energy harvesting (Akbar et al., 2022; Akbar and Curiel-Sosa et, 2019) and aerofracturelasticity (Abdullah et al., 2019; 2018). In the current work, a RANS based on Finite Volume Method (FVM) coupled with Finite Element Method (FEM) is utilized. The implementation of FVM is proposed to capture the change in flow contours around the wing structures as it could not be captured by panel-based method, i.e., DLM.

The present investigation is an extension of the work by Moelyadi and Zulkarnain (2021) regarding the design of a high-altitude long-endurance (HALE) UAV. A new investigation in terms

of an operational flight condition is also evaluated. A cruising operation with gust wind disturbance is studied. Simulation is carried out using the two-way fluid-structure interaction (FSI) method. The fluid flow solution will be solved in the Computational Fluid Dynamics (CFD) domain, which has been widely used in various problems, i.e., open channel wind turbines (Darmawan and Tanujaya, 2019; Sudarsono et al., 2019) and ships/boats (Riyadi et al., 2022; Dwiputera et al., 2022). On the other hand, the structural solution is solved in the Computational Structural Dynamics (CSD) domain using Finite Element Method (FEM). Because of the complexity of the phenomena, two independent wings are modeled in a rigid-flexible configuration. Various discrete 1-cosine gust velocities are created and considered in occurrence probability. Validations are carried out numerically and compared to the historical experiment data.

2. Mathematical Model

In this section, a mathematical model of fluid-structure coupling under disturbance that is used in the simulation is presented. Firstly, the mathematical model from the fluid solution needs to be investigated based on its operational condition. In very low-speed flight of HALE, the flow appears at a low Reynolds number or generally laminar, which is easy to separate. However, the inclusion of kinetic momentum energy from the freestream flow may lead to the reattachment of separated flow, inducing turbulence and forming what is commonly referred to as a "separation bubble". Therefore, fluid solution requires equations that can model both laminar and turbulent regions (Winslow et al., 2018). The problems can be solved using the Unsteady Navier-Stokes equation shown by (1) and (2). The assumptions, including transient, incompressible, no heat transfer, and the presence of a viscous effect on the surface of the wing, are used (Wendt et al., 2009).

$$\frac{\partial \rho_f}{\partial t} + \rho_f \frac{\partial (v_i)}{\partial x_i} = 0 \tag{1}$$

$$\rho_f \frac{\partial v_i}{\partial t} + \rho_f \frac{\partial (v_i v_j)}{\partial x_j} = -\frac{\partial P}{\partial x_i} + \mu \frac{\partial}{\partial x_j}\left(\frac{\partial v_i}{\partial x_j} + \frac{\partial v_j}{\partial x_i}\right) + \mu \frac{\partial}{\partial x_k}\left(\frac{\partial v_i}{\partial x_k} + \frac{\partial v_k}{\partial x_i}\right) \tag{2}$$

In the CFD domain, there are several numerical methods to compute the Navier-Stokes equation, such as Large Eddy Simulation (LES) and Reynold Averaged Navier Stokes (RANS). In this work, DES (Detached Eddy Simulation) combines both RANS and LES models as a hybrid equation. RANS is used close to the boundary layer, while LES is in the wake region. The advantage of this hybrid formulation is that it can compute turbulent flow with large eddy sizes while maintaining less computational time than using the LES method in the whole model. The solver is using DES with a turbulent SST model. The SST-DES model was introduced by Strelets by changing the SST-RANS model to LES in the Lt turbulent size parameter (Strelets et al., 2001; Menter, 1994).

In the CSD domain, the spring model approach is used to investigate the response of the wing. The model that also consists of aerodynamics flow can be written in Equation (3)

$$[M_s - M_f]\{\ddot{U}\} + [C_s - C_f]\{\dot{U}\} + [K_s - K_f]\{U\} = \{F_{disturbance}(t)\} \tag{3}$$

Where the variable with the subscript 's' is a property of the structure, while the subscript 'f' is a property of the fluid; $\{U\}$ is the nodal displacement vector; $\{\dot{U}\}$ is the nodal velocity vector; $\{\ddot{U}\}$ nodal acceleration vector; $\{F_{disturbance}(t)\}$ is an external disturbance in the form of force as a time function (Akbar et al., 2022). If the disturbance F on the right side is removed, then Equation (3) will become an aeroelastic problem such as flutter and divergence. The displacement parameter from the spring model can be solved numerically using Newmark time integration and Hilber-Hughes-Taylor (HHT) methods. This is an implicit method where each time step can be solved simultaneously (Tabatabaei et al., 2020).

Equations from the fluid (CFD) and the structural (CSD) domains will be solved in each module. An FVM and FEM-based commercial software, ANSYS CFX and ANSYS Mechanical are utilized. The results of the computation are forced from the integration of pressure distribution and

structural deformation, respectively. Each set of data will be transferred and interpolated between the various modules through a System Coupling mechanism until convergence is achieved or the coupling step limit is reached. As illustrated in Figure 1, these processes will be carried out at each time step.

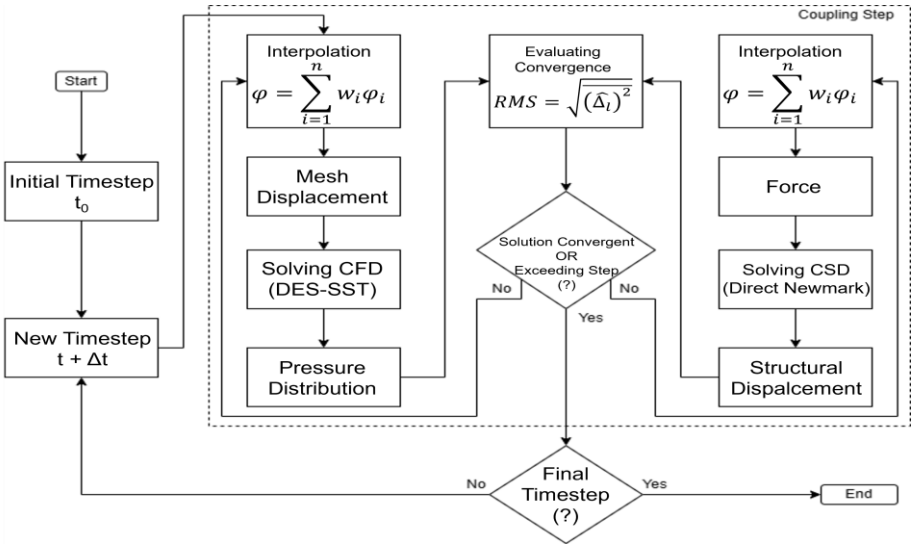

Figure 1 Two-way fluid structure interaction numerical flowchart

3. Simulation Methodology

In the present work, the tandem wing configuration of Moelyadi and Zulkarnain (2021) is simplified without the boom. The front wing is modeled as rectangular with winglets, while the rear wing is rectangular and tapered closer to the tip. Both wings are constructed using K3311 airfoil for a low Reynolds number regime.

Table 1 Fluid properties at sea level

Temperature (T) (K)	288.15
Pressure (P) (Pa)	101325
Fluid Density (ρ_f) (kg/m3)	1.225
Dynamic Viscosity (μ) (Pa.s) (10^5)	1.821

Table 2 Rear wing material properties

Structural Density (ρ_s) (kg/m3)	17.4
Young Modulus (E) (GPa)	1.5
Poisson's Ratio (ν)	0.3
Shear Modulus (G) (GPa)	0.6

The fluid domain model is created using ANSYS CFX from the Fluid Flow module. Both geometries are set in the middle of the domain, and the root section coincides with the symmetry surface. Figure 2 (a) shows the computational domains created. Structured mesh consists of a combination of H grid and C grid topology, which is used to reduce computational time and make it easier to manage grid distribution. In addition to this simulation, the unstructured mesh is also used as validation, as shown in Figure 2 (b), and will be used in FSI simulation if the deformation is very large and might cause error due to negative volume in the structured mesh. Validation of the FSI simulation results between structured and unstructured mesh will be explained in the next section.

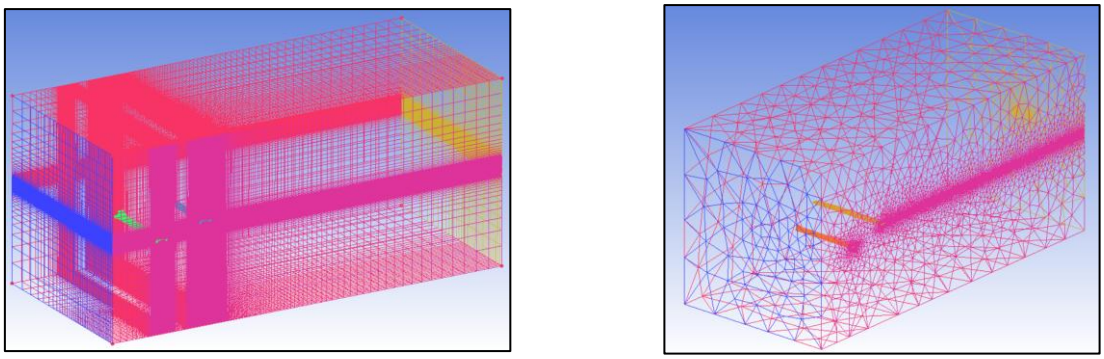

(a) (b)

Figure 2 Mesh on the fluid domain: (a) Structured, and (b) Unstructured

The fluid domain is assumed to be stationary, therefore, air will be generated from the inlet in the parallel and perpendicular direction chordwise. Perpendicular wind speed is assumed to be a disturbance known as a vertical gust. Vertical velocity variation is modeled in 1-cosine gust based on ESDU regulations 04024 (ESDU, 2004). Gust velocity can be written as depicted in Equation (4)

$$U = \frac{U_g}{2}\left(1 - \cos\frac{\pi s}{H}\right) \tag{4}$$

where H is the horizontal distance from zero gust velocity to the maximum value of 12.5 of the chord length, because the plane in the simulation does not move, but the air flows through it. Therefore, the gust disturbance will also come from the inlet and the freestream velocity. Gust modeling in the CFD domain needs to be defined in the time domain through Equation (5)

$$s = \frac{V_f t}{c} \tag{5}$$

where V_f is the freestream speed, Gust will be generated for 2.125 seconds, as seen at Figure A.1 in Appendix A. In addition, the gust speed is varied by changing its amplitude from 0.5, 1, 2, 3, and 4 m/s. However, it should be noted that, in real conditions, gusts passing through the aircraft can occur continuously, with highly varying amplitudes of speeds. When determining the frequency of gusts appearing at a certain speed amplitude, it can be calculated in terms of relative frequency. ESDU 69023 shows empirical results based on historical aircraft data at various altitudes (ESDU, 1989).

The next step is defining atmospheric conditions and boundary conditions in the fluid domain. Table 1 shows the atmospheric conditions at sea level. Air is assumed to be isothermal because the temperature difference between the wing and the environment in the fluid domain is very small, viscous forces are dominant closer to the surface of the wing, and incompressible. Dynamic mesh is used in the region closer to the rear wing. Detached Eddy Simulation (DES) - Shear Stress Transport (SST) is used to calculate flow around the boundary layer and wake region. Simulation in CFX has six boundary conditions, as shown in Figure 3. The inlet is defined at the front of the fluid domain, defined as the combination of horizontal velocity 10 m/s and vertical gust velocity based on Figure A.1 starting from 0.5 seconds until rest. Outlet is defined as zero relative static pressure and it is located at the end of the computational domain. Fairfield is defined as the opening pressure and it is located at the top, bottom, and adjacent to the rear wing tip surface. Symmetry is defined as the mirror of the computational domain because this simulation consists of a half-model wing geometry. A rigid front wing is defined as a no-slip wall, while a deformed rear wing is defined as a coupling geometry to the structural model.

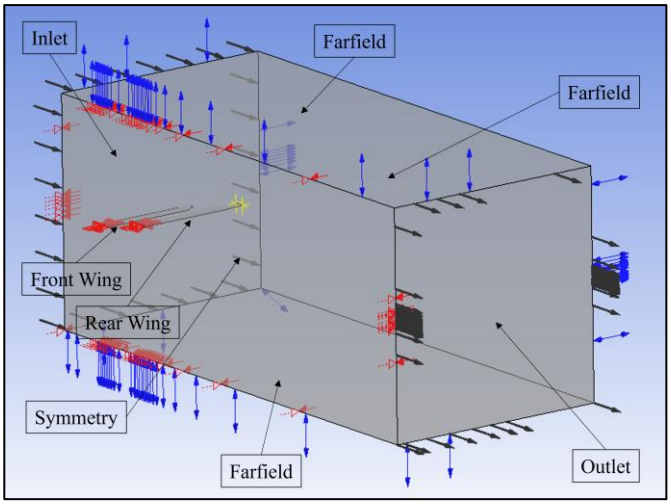

Figure 3 Boundary conditions of the fluid domain

The structural domain model is created using ANSYS Mechanical from the Transient Structural module. The front wing is assumed to be rigid; therefore, it is not included in the structural analysis. The rear wing is assumed to have solid and homogeneous material properties. Structural properties that will be used as input parameters are density, elastic modulus, and Poisson's ratio, as shown in Table 2. Boundary conditions in the HALE wing structure are fixed support on the wing root surface and fluid-solid interface on the other wing surfaces, as shown in Figure 4. In addition, the damping of the structure is removed, and as a result, the decaying of the deflection only depends on fluid flow.

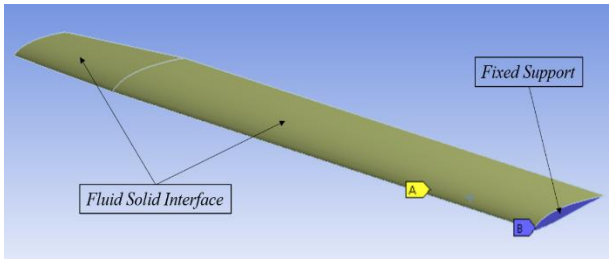

(a)

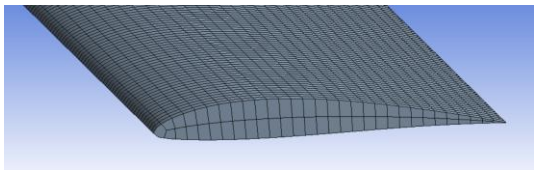

(b)

Figure 4 Computational Structural Domain: (a) Boundary conditions, and (b) Mesh

Data exchange between fluid computation (CFD) and structure (CSD) domains in FSI simulations performed using the two-way fluid-structure interaction (FSI) method is set to System Coupling. The setup section of the Transient Structural and Fluid Flow modules is connected to the System Coupling to exchange data between the fluid simulation and the wing model structure via the interface. The simulation time and timestep in the analysis configuration are set according to the Transient Structural and Fluid Flow setups. The simulation was carried out for 5 seconds with a time change of 0.005 seconds.

4. Validation

This section will discuss validation regarding the FSI simulation that has been conducted. Validations include mesh independence in both CFD and CSD modules as well as experimental comparison.

4.1. Mesh Independence Validation

Structural domain validation was carried out numerically and experimentally. Mesh independence is a necessary numerical validation to reduce computational errors because of poor

models. Parameters that have been used to determine whether the number of elements is sufficient were the vibration mode of the first bending, second bending, and first torsion, according to Figure B.1 (a) in Appendix B. In the Computational Structural Domain (CSD), based on computational time and accuracy, the rear wing consists of 14551 elements. Fluid domain validation is also carried out numerically using an independence test. In Computational Fluid Domain (CFD), based on the results of the numerical simulation at steady state in Figure B.1 (b) and considering computational capabilities and simulation stability, the number of elements in the structured mesh that would be used in the FSI simulation was 4.3 million.

4.2. Experimental Validation

The structural model was also validated by conducting an experimental static test. Additional mass was distributed along the wing as the replacement of aerodynamic load. In the numerical simulation, point mass was added at the top of the wing and affected by earth gravitational in 1g and 1.5g. Figure B.2 in Appendix B shows a comparison of static deflection in experimental and numerical simulations. Structural deformation along the span was different but had a similar trend and order. Therefore, the modeled rear wing structure could be used for this FSI simulation.

4.3. Fluid-Structure Interaction Model Validation

Fluid-Structure Interaction simulation is also used in several validation. Firstly, a comparison between unstructured and structured mesh in the fluid domain is evaluated to prove consistent results regarding structural deformation. Figure B.3 in Appendix B shows the deflection of the wing tip during simulation time with variations in the amplitude of the gust velocity and the type of mesh in the fluid domain. There are no significant differences in terms of tip deflection between the two types of mesh for each case; therefore, both fluid models can also be used in this simulation.

5. Fluid-Structure Interaction Response Analysis

The interaction between the fluid and the wing structure produces an oscillatory (heaving) motion. The simulation starts from conditions without airflow, and then the flexible rear wing will be deflected due to the lift generated by the difference in pressure distribution on the top and bottom of the wing until it reaches the first second, which can be called the initial deflection. On the other hand, the gust is generated at 0.5 seconds and needs to travel around 0.75 seconds before it reaches the front wing.

5.1. Analysis of Fluid-Structure Interaction in High Occurrence Gust

This section presents an FSI simulation of a tandem wing configuration subjected to gust disturbances with amplitudes of 0.5 and 1 m/s. These disturbances occurred more than ten times during the flight. Figure 5 illustrates the deflection of the rear wing tip. The appearance of gust in the form of perpendicular flow to the chord direction results in an additional deflection of the flexible rear wing. The change in the position of the rear wing tip follows the 1-cosine gust shape, although there is an insignificant difference in time (phase lag) between the increase in gust and the deflection of the wing.

The additional deflection of the rear wing can be explained in terms of the FSI coupling phenomenon between the computational fluid (CFD) and structure (CSD) domains. Gust that emerges from the inlet will change the resultant direction of flow passing through the two wings, where the change in direction will form an angle between the flow direction and the chord of the wing, which is called the angle of attack. Increasing the angle of attack on the rear wing up to 2.8 and 5.7 degrees for the two-parameter variations will change the pressure distribution along the wing span, which is integrated into aerodynamic forces, so that the wing deflection becomes larger, which in turn will change the flow around it. Figure 6 shows changes in the lift forces during the FSI simulation. Positive vertical flow increases lift and drag, which results in greater wing tip deflection, Besides that, the moment in the spanwise direction gives the wing a tendency to pitch

down. Similar to changes in rear wing tip deflection, lift force also experiences changes following the 1-cosine gust shape, even though there is an insignificant difference in time (phase lag).

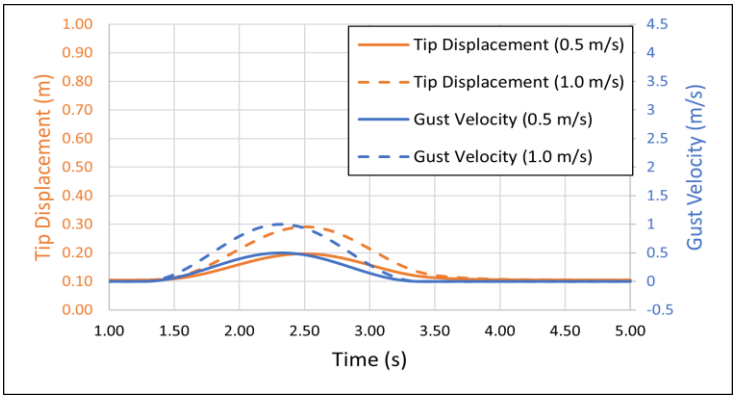

Figure 5 Rear wing tip deflection at 0.5 and 1.0 m/s gust amplitude

The FSI simulation results are also shown by contours in the computational fluid (CFD) and structure (CSD) domains to understand more clearly the phenomena that occur, as shown at Figure C.1 in Appendix C. The streamline changes with time due to the vertical velocity passing through the two wings. As long as the gust effect takes place, the change in the maximum angle of attack for both parameters has not reached the stall area, so the flow separation will not occur. The front wing is assumed to be rigid, so changes in aerodynamic forces caused by changes in the angle of attack will not change the overall position of the wing. As for the flexible rear wing, changes in wing position along the span are only caused by changes in the angle of attack without changing the attitude of the pitch. This is due to the torsional stiffness being able to withstand the pitch moment that appears on the wing. On the other hand, there is no interaction between the downstream flow of the front wing and the upstream rear wing even when the vertical gust speed is maximum, or the wingtip deflection is maximum. Therefore, the additional deflection that arises due to changes in lift force is only due to gust originating from the inlet.

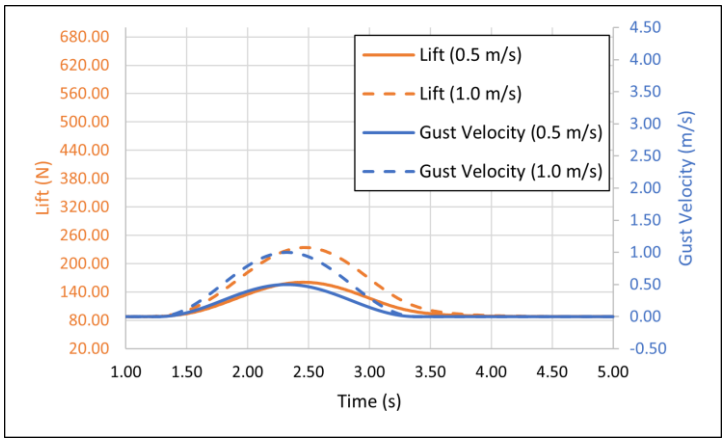

Figure 6 Lift response at 0.5 and 1.0 m/s gust amplitude

5.2. Analysis of Fluid-Structure Interaction in Low Occurrence Gust

This section describes FSI simulations of tandem wings with extreme conditions of gust disturbances at amplitudes of 2, 3, and 4 m/s that occur less than ten times during flight. The deflection of the rear wing tip is shown in Figure 7, where the deflection of the rear wing tip no longer follows the 1-cosine gust shape. In the case of 2 m/s, the change in rear wingtip deflection is similar to that of the gust profile, although it looks more sloping in the amplitude region. However, in cases of 3 and 4 m/s, the deflection gradient experienced significant changes in the

peaks and difference in time (phase lag) between the increase, peak, and decrease in vertical gust speed and wing deflection. The phenomenon of FSI coupling between the computational fluid (CFD) and structure (CSD) domains with vertical flow disturbance can be explained as follows. Gust that emerges from the inlet will change the direction of the resultant flow through the two wings, where changes in the angle of attack will change the pressure distribution between the upper and lower surfaces of the wings, which are integrated into aerodynamic forces. For the three relatively extreme conditions, the addition of the angle of attack on the rear wing reaches 11.3, 16.9, and 21.8 degrees, respectively. Figure 8 shows changes in the lift force during the FSI simulation. Positive vertical flow increases lift and drag, which results in greater wing tip deflection, Besides that, the moment in the spanwise direction gives the wing a tendency to pitch down. However, similar to the deflection response of the rear wing tip, aerodynamic forces and moments also experience a phase lag and significant gradient changes in the peaks and decreases of gust.

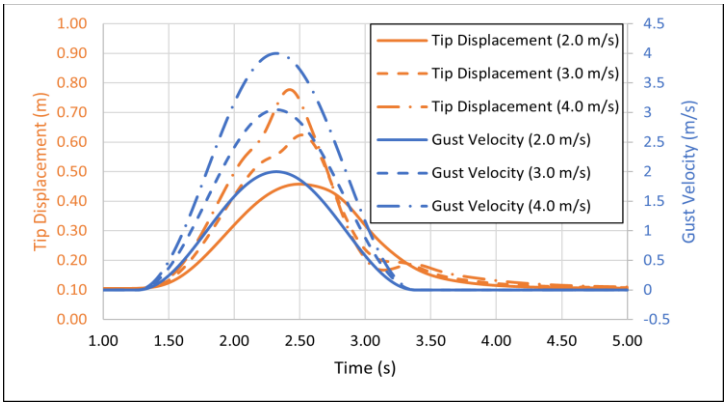

Figure 7 Rear wing tip deflection at 2.0, 3.0, and 4.0 m/s gust amplitude

The FSI simulation results are also shown by contours in the fluid domain (CFD) and structure (CSD) to find out more clearly the phenomena that occur, as shown at Figure C.2 in Appendix C. At the maximum speed of the gust, the flow separation on the upper surfaces at the front and rear wings is caused by the angle of attack reaching the stall area. In addition, the interaction between the downstream of the forewing and the upstream of the hindwing occurs on the lower surface. The flow originating from the front wing in the form of a wake affects the distribution of pressure on the lower surface of the rear wing before separation occurs on the upper surface.

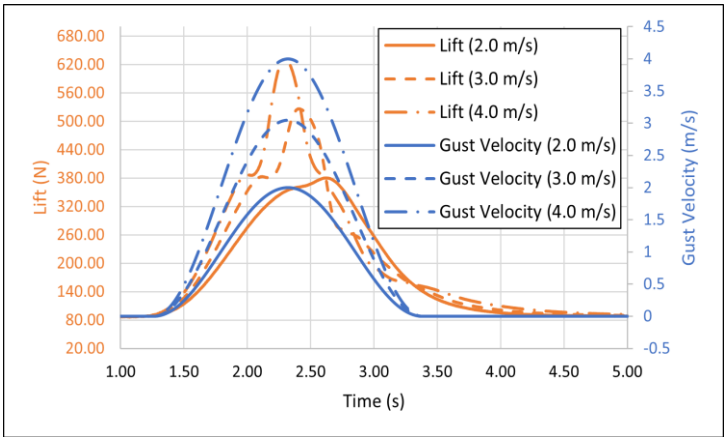

Figure 8 Lift response at 2.0, 3.0, and 4.0 m/s gust amplitude

6. Conclusions

A new investigation on the FSI phenomenon of a tandem wing configuration has been conducted in this work. A two-way FSI by means of coupling between CFD and CSD has been implemented. The effect of gust disturbances on the structural responses of the tandem wings has been evaluated. In addition to the response exerted by the gust, the influence of the wake generated from the front wing to the rear wing has also been observed. In the present works, a 1-cosine discrete gust is applied with a gust amplitude of up to 4 m/s. Based on the results of the numerical investigation, when the wings are excited by a small gust amplitude, the pattern of the structural response closely follows the function of the gust with respect to time. In contrast, if a higher gust amplitude is applied, the structural response has some discrepancies with the gust patterns and depicts a sharper trend toward its peak value. The phenomenon is caused by a high change of angle of attack; therefore, a larger flow separation occurs when a higher gust exerts the wing. Nonetheless, it is important to note that the likelihood of encountering high gust amplitudes is relatively low, potentially resulting in a frequency of less than one occurrence per flight. Therefore, for a more realistic representation that considers a higher probability of encountering gusts, the structural response pattern closely resembles that of a 1-cosine gust shape.

Acknowledgements

The authors wish to acknowledge the funding provided via the ITB Research, Community Service and Innovation Program (P2MI ITB) 2023.

Author Contributions

David Waldo Parlindungan and Mochammad Agoes Moelyadi conceived of the presented Idea. David Waldo Parlindungan performed the computations and verified the methodologies. All authors discussed the results and contributed to the final manuscript.

Conflict of Interest

All authors declare that they have no conflicts of interest.

References

Abbey, S, Dankhara, K & Senthilkumar, S 2020, 'Aerodynamic characteristics of flow over two unsymmetrical tandemly arranged airfoils – numerical simulation', *IOP Conference Series: Materials Science and Engineering*, vol. 912, article 042033, https://doi.org/10.1088/1757-899X/912/4/042033

Abdullah, NA, Akbar, M, Wirawan, N & Curiel-Sosa, JL 2019, 'Structural integrity assessment on cracked composites interaction with aeroelastic constraint by means of XFEM', *Composite Structures*, vol. 229, p. 111414, https://doi.org/10.1016/j.compstruct.2019.111414

Abdullah, NA, Curiel-Sosa, JL & Akbar, M 2018, 'Aeroelastic assessment of cracked composite plate by means of fully coupled finite element and doublet lattice method', *Composite Structures*, vol. 202, pp. 151-161, https://doi.org/10.1016/j.compstruct.2018.01.015

Akbar, M & Curiel-Sosa, JL 2019, 'An iterative finite element method for piezoelectric energy harvesting composite with implementation to lifting structures under gust load conditions', *Composite Structures*, vol. 219, pp. 97-110, https://doi.org/10.1016/j.compstruct.2019.03.070

Akbar, M, Ramadhani, MJ, Izzuddin, MA, Gunawan, L, Sasongko, RA, Kusni, M & Curiel-Sosa, JL 2022, 'Evaluation on piezoaeroelastic energy harvesting potential of a jet transport aircraft wing with multiphase composite by means of iterative finite element method', *International Journal of Technology*, vol. 13, no. 4, pp. 803-813, https://doi.org/10.14716/ijtech.v13i4.5468

Arranz, G, Flores, O, & García-Villalba, M 2020, 'Three-dimensional effects on the aerodynamic performance of flapping wings in tandem configuration', *Journal of Fluids and Structures*, vol. 94, article 102893, https://doi.org/10.1016/j.jfluidstructs.2020.102893

Bie, D, & Li, D 2022, 'Numerical analysis of the wing–wake interaction of tandem flapping wings in forward flight', *Aerospace Science and Technology*, vol. 121, article 107389. https://doi.org/10.1016/j.ast.2022.107389

Bravo-Mosquera, PD, Catalano, FM & Zingg, DW 2022, 'Unconventional aircraft for civil aviation: A review of concepts and design methodologies', *Progress in Aerospace Sciences*, vol. 131, p. 100813, https://doi.org/10.1016/j.paerosci.2022.100813

Broering, T M, & Lian, Y 2015, 'Numerical study of tandem flapping wing aerodynamics in both two and three dimensions', *Computers & Fluids*, vol. 115, pp. 124–139. https://doi.org/10.1016/j.compfluid.2015.04.003

Chou, H, Liu, Y, & Hsiao, F 2013, 'The Aerodynamic behavioral Study of Two Wing's Wake Flow in Tandem Arrangement', *Procedia Engineering*, vol. 67, pp. 1–14. https://doi.org/10.1016/j.proeng.2013.12.001

Darmawan, S & Tanujaya, H 2019, 'CFD investigation of flow over a backward-facing step using an RNG k-ε turbulence model', *International Journal of Technology*, vol. 10, no. 2, pp. 280-290, https://doi.org/10.14716/ijtech.v10i2.800

Dhital, K, Nguyen, AT & Han, J-H 2022, 'Aeroelastic modelling and analysis of wings in proximity', *Aerospace Science and Technology*, vol. 130, p. 107955, https://doi.org/10.1016/j.ast.2022.107955

D'Oliveira, FA, De Melo, FCL & Devezas, CT 2016, 'High-altitude platforms - present situation and technology trends', *Journal of Aerospace Technology and Management*, vol. 8, no. 3, pp. 249-262, https://doi.org/10.5028/jatm.v8i3.699

Dwiputera, H, Prawira, NY, Andira, MA & Budiyanto, MA 2020, 'Effect of angle of attack variation of stern foil on high-speed craft on various speed with computational fluid dynamics method', *International Journal of Technology*, vol. 11, no. 7, pp. 1359-1369, https://doi.org/10.14716/ijtech.v11i7.4467

ESDU 1989, 'Average gust frequencies subsonic transport aircraft', *Engineering Sciences Data Unit*, item no. 69023

ESDU 2004, 'An introduction to rigid aeroplane response to gusts and atmospheric turbulence', *Engineering Sciences Data Unit*, item no. 04024

Feistel, TW, Corsiglia, VR & Levin, DB 1981, 'Wind-tunnel measurements of wing-canard interference and a comparison with various theories', *SAE Transactions*, vol. 90, no. 2, pp. 2026-2039, https://www.jstor.org/stable/44632758

Goetzendorf-Grabowski, T 2023, 'Flight dynamics of unconventional configurations', *Progress in Aerospace Sciences*, vol. 137, p. 100885, https://doi.org/10.1016/j.paerosci.2023.100885

Gong, WQ, Jia, BB & Xi, G 2016, 'Experimental study on instantaneous thrust and lift of two plunging wings in tandem', *Experimental Fluids*, vol. 57, pp. 1-11, https://doi.org/10.1007/s00348-015-2096-2

Jones, R, Cleaver, D & Gursul, I 2015, 'Fluid-structure interactions for flexible and rigid tandem-wings at low Reynolds numbers', in *53rd AIAA Aerospace Sciences Meeting*, Florida, USA, https://doi.org/10.2514/6.2015-1752

Khan, FA & Mueller, TJ 1991, 'Tip vortex/airfoil interaction for a low Reynolds number canard/wing configuration', *Journal of Aircraft*, vol. 28, no. 3, pp. 181-186, https://doi.org/10.2514/3.46010

Kirschmeier, B & Bryant, M 2018, 'Experimental investigation of wake-induced aeroelastic limit cycle oscillations in tandem wings', *Journal of Fluids and Structures*, vol. 81, pp. 309-324, https://doi.org/10.1016/j.jfluidstructs.2018.04.015

Martínez-Muriel, C., García-Villalba, M., & Flores, O 2024, 'On the role of wake-capture and resonance in spanwise-flexible flapping wings in tandem', *Journal of Fluids and Structures*, vol. 130, article 104175, https://doi.org/10.1016/j.jfluidstructs.2024.104175

Menter, FR 1994, 'Two-equation eddy-viscosity turbulence models for engineering applications', *AIAA Journal*, vol. 32, no. 8, pp. 1598-1605, https://doi.org/10.2514/3.12149

Moelyadi, MA & Zulkarnain, MF 2021, 'HALE UAV ITB perpetual flight', *IOP Conference Series: Materials Science and Engineering*, vol. 1109, p. 012028, https://doi.org/10.1088/1757-899X/1109/1/012028

Noll, TE, Brown, JM, Perez-Davis, ME, Ishmael, SD, Tiffany, GC & Gaier, M 2004, *Investigation of the Helios prototype aircraft mishap,* NASA Mishap Report, NASA, Washington, DC

Qin, J., Zhou, Z., Yang, G., Shao, Z., & Zong, J 2024, 'Aero-propulsive coupling modeling and dynamic stability analysis of distributed electric propulsion tandem-wing UAV with rapid ascent capability', *Aerospace Science and Technology*, vol 153, article 109406. https://doi.org/10.1016/j.ast.2024.109406

Riyadi, S, Aryawan, WD & Utama, IKAP 2022, 'Experimental and computational fluid dynamics investigations into the effect of loading condition on resistance of hard-chine semi planning crew boat', *International Journal of Technology*, vol. 13, no. 3, pp. 518-532, https://doi.org/10.14716/ijtech.v13i3.4597

Scharpf, DF & Mueller, TJ 1992, 'Experimental study of a low Reynolds number tandem airfoil configuration', *Journal of Aircraft,* vol. 29, no. 2, pp. 231-236, https://doi.org/10.2514/3.46147

Shah, SHR & Ahmed, A 2022, 'Experimental investigation of wings in tandem', *In:* AIAA AVIATION 2022 Forum, Chicago, USA, https://doi.org/10.2514/6.2022-3391.vid

Strelets, M 2001, 'Detached eddy simulation of massively separated flows', *In:* 39th Aerospace Sciences Meeting and Exhibit, Reno, USA, https://doi.org/10.2514/6.2001-879

Sudarsono, S, Susastriawan, AA & Sugianto, S 2019, 'Three-dimensional CFD analysis of performance of small-scale HAWT based on modified NACA-4415 airfoil', *International Journal of Technology,* vol. 10, no. 1, pp. 212-221, https://doi.org/10.14716/ijtech.v10i1.2237

Tabatabaei Malazi, M, Eren, ET, Luo, J, Mi, S & Temir, G 2020, 'Three-dimensional fluid–structure interaction case study on elastic beam', *Journal of Marine Science and Engineering*, vol. 8, no. 9, p. 714, https://doi.org/10.3390/jmse8090714

Wendt, JF 2009, *Computational fluid dynamics - an introduction*, Springer, Berlin

Winslow, J, Otsuka, H, Govindarajan, B & Chopra, I 2018, 'Basic understanding of airfoil characteristics at low Reynolds numbers (104–105)', Journal of Aircraft, vol. 55, no. 3, pp. 1050–1061, https://doi.org/10.2514/1.C034415

Yang, X., Luo, Y., Lang, X., & Wang, W 2024, 'Investigation of the aerodynamic performance of the dragonfly-inspired tandem wings considering the coupling between the stroke plane and phase difference', *Aerospace Science and Technology*, vol. 155, article 109717. https://doi.org/10.1016/j.ast.2024.109717